Metallic phase in the two-dimensional ionic Hubbard model

K. Bouadim[1], N. Paris[2], F. Hébert[1], G.G. Batrouni[1], and R.T. Scalettar[2]
[1] *INLN, Université de Nice Sophia–Antipolis, CNRS; 1361 route des Lucioles, 06560 Valbonne, France and*
[2] *Physics Department, University of California, Davis, California 95616, USA*

We investigate the phases of the ionic Hubbard model in a two-dimensional square lattice using determinant quantum Monte Carlo (DQMC). At half-filling, when the interaction strength or the staggered potential dominate we find Mott and band insulators, respectively. When these two energies are of the same order we find a metallic region. Charge and magnetic structure factors demonstrate the presence of antiferromagnetism only in the Mott region, although the externally imposed density modulation is present everywhere in the phase diagram. Away from half-filling, other insulating phases are found. Kinetic energy correlations do not give clear signals for the existence of a bond-ordered phase.

PACS numbers: 71.10.Fd, 71.30.+h, 02.70.Uu

I. INTRODUCTION

Tight binding models, such as the Hubbard Hamiltonian, have been widely studied for their ability to describe different kinds of insulating phases present in condensed matter systems. Interactions between fermions give rise to gapped Mott insulators where the fermions are immobile at commensurate fillings. For bipartite lattices, Mott behavior is typically associated with antiferromagnetic order. On the other hand, the imposition of an external periodic potential can drive band insulating behavior. In systems where several types of insulating effects are present, phase transitions can take place as the relative strength of the parameters is changed. Close to such transitions, the competition between these different terms allows smaller effects, such as kinetic energies, to result in low temperature metallic phases or more exotic types of correlations such as bond-order. Such compensating effects are believed to explain enhanced response in different quasi-one-dimensional systems such as organic materials[1], ferroelectric perovskites[2] or transition metal-oxides[3].

A simple model exhibiting this kind of behavior is the ionic Hubbard Hamiltonian[4], a tight binding model that includes an on-site repulsion and a staggered potential that takes alternating values on neighboring sites of a bipartite lattice. At half-filling, the on-site repulsion drives the system into an antiferromagnetic Mott insulator (MI), with a homogeneous density. When the staggered potential dominates, a band insulator (BI) with a regular modulation of the density results. A quantum phase transition between these two states occurs in the phase diagram.

In one dimension, the ionic Hubbard model has been widely studied through a variety of techniques including density matrix renormalization group (DMRG), exact diagonalization, bosonization and quantum Monte Carlo (QMC) with on-site[5,6,7,8] or extended[2,3,9,10,11,12] interactions. The precise conclusions are still subject to some debate, but many of the studies suggest that the direct transition from the band insulator to the Mott insulator is replaced by an intervening insulating bond-ordered phase. In two dimensions, dynamical mean field theory (DMFT)[13], cluster-DMFT[14] and determinant quantum Monte Carlo (DQMC)[15] were used. The existence of an intermediate phase between the BI and MI phases has been established, as in one dimension, but the precise nature of the phase is still under debate (see section II). Studies of a bilayer Hubbard model[17] and in infinite dimension[18] yield similar results with a low temperature metal as the intermediate phase. Here the interplanar coupling, if sufficiently large, gives a noninteracting band structure with a gap at half-filling much like a staggered potential. A recent experiment attempts to observe this kind of phase[19].

A related problem is the study of heterostructures of $SrTiO_3$ and $LaTiO_3$, one being a MI, the other a BI and a metallic phase appearing at the interface between the two[20]. Some of the phenomena presented here also have similarities with those found in corresponding disordered models used to describe binary alloys[21].

In this paper, we consider the different phases and transitions of the ionic Hubbard Hamiltonian on a two-dimensional square lattice using determinant quantum Monte Carlo (DQMC), extending our initial study[15]. In section II, we introduce the model and summarize our previous results. In section III, we briefly describe the numerical techniques used while in section IV, we investigate further the different phases by measuring the charge and magnetic structure factors and the spectral function. We then present an analysis of the properties away from half filling (section V) and the search for bond-order waves (section VI). Conclusions are in section VII.

II. FERMIONS IN A STAGGERED POTENTIAL

We consider the ionic Hubbard model

$$\hat{H} = -t \sum_{\langle \mathbf{r}\mathbf{r}'\rangle\sigma} (c^\dagger_{\mathbf{r}\sigma} c_{\mathbf{r}'\sigma} + c^\dagger_{\mathbf{r}'\sigma} c_{\mathbf{r}\sigma}) + U \sum_{\mathbf{r}} n_{\mathbf{r}\uparrow} n_{\mathbf{r}\downarrow} + \sum_{\mathbf{r}} \left[\frac{\Delta}{2} (-1)^{(x+y)} - \mu \right] (n_{\mathbf{r}\uparrow} + n_{\mathbf{r}\downarrow}) \quad (1)$$

where $c^\dagger_{\mathbf{r}\sigma}(c_{\mathbf{r}\sigma})$ are the usual fermion creation (destruction) operators on site $\mathbf{r} = (x, y)$ of a two-dimensional square lattice with spin σ and where $n_{\mathbf{r}\sigma} = c^\dagger_{\mathbf{r}\sigma} c_{\mathbf{r}\sigma}$ is the number operator. The hopping parameter, t, sets the energy scale and is fixed at a value of 1, while tuning the chemical potential μ gives the desired fermion filling. The interaction strength U and staggered potential $(-1)^{(x+y)}\,\Delta/2$ are the two competing terms of our system, the former encouraging single occupancy of all sites and the latter double occupancy of the low energy sublattice.[16]

Considering the limiting cases $U \gg \Delta$ and $\Delta \gg U$ we find two distinct insulating phases at half-filling (density $\rho = 1$). For $\Delta = 0$, the usual translationally invariant Hubbard model arises and, at $T = 0$, forms an antiferromagnetic Mott insulator at half-filling for any value of U. At strong coupling, the gap is set by U, while the effective anti-ferromagnetic coupling is set by $J = 4t2/U$. These two energy scales are evident in the magnetic properties where $T \sim U$ demarks the onset of moment formation on individual sites and $T \sim J$, the onset of antiferromagnetic order between sites.

In the non interacting limit $U = 0$, the Hamiltonian can be diagonalized in Fourier space (where it reduces to a set of independent 2×2 matrices)

$$\hat{H} = \sum_{\mathbf{k},\sigma} E_{\mathbf{k}}\, c^\dagger_{\mathbf{k}\sigma} c_{\mathbf{k}\sigma} \quad \text{with} \quad E_{\mathbf{k}} = \pm\sqrt{\epsilon_{\mathbf{k}} 2 + (\Delta/2) 2}$$

where the sum runs over half the Brillouin zone and where $\epsilon_{\mathbf{k}} = -2t\,(\cos(k_x) + \cos(k_y))$ is the energy of a free particle of wave vector $\mathbf{k} = (k_x, k_y)$. The eigenenergies $E_{\mathbf{k}}$ are then split into two bands separated by a gap Δ and, in this limit, the system is a band insulator at half-filling. These two insulating phases can be seen schematically in Fig. 1.

Recently, it was shown[13,14,15] that there is no direct transition between these two insulating phases, but that an intermediate phase appears (Fig. 2). The precise nature of the phase is still being debated. In previous work[15], we used the determinant quantum Monte Carlo algorithm (DQMC) to study the conductivity of the model. Performing a finite size and temperature analysis, we concluded that the intermediate phase has a finite conductivity and is, consequently, metallic. Garg *et al.* arrive at the same conclusion in their dynamical mean field theory (DMFT) study[13] while using a cluster-DMFT analysis, Kancharla *et al.* argue for a bond ordered wave (BOW) phase[14].

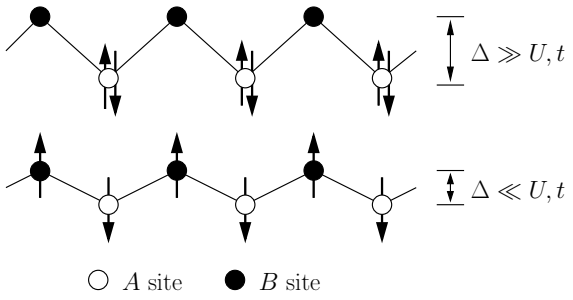

FIG. 1: Schematic diagram of electrons in a staggered potential. The A sites have lower chemical potential than the B sites (the difference being Δ). For low interaction strength $U \ll \Delta$, the electrons prefer to doubly occupy the A sites and form a band insulator. For $U \gg \Delta$, it is favorable to have only one electron per site and to form a Mott insulator. The hopping term t then generates an antiferromagnetic modulation.

III. COMPUTATIONAL METHODS

DQMC[22] is a numerical approach which expresses the partition function $Z = \mathrm{Tr}\,\exp(-\beta H)$ as a path integral where the inverse temperature β is discretized. The interaction term is decoupled via a Hubbard-Stratonovich (HS) transformation, introducing a sum over an Ising spin field and leaving the Hamiltonian in a quadratic form with respect to the fermion operators. The fermionic degrees of freedom can then be integrated out and the remaining Boltzmann weight is expressed as the determinant of the product of two matrices that depend on the HS spin variables. In the conventional Hubbard model, this determinant is positive at half-filling, due to particle-hole symmetry. With the staggered potential, the deter-

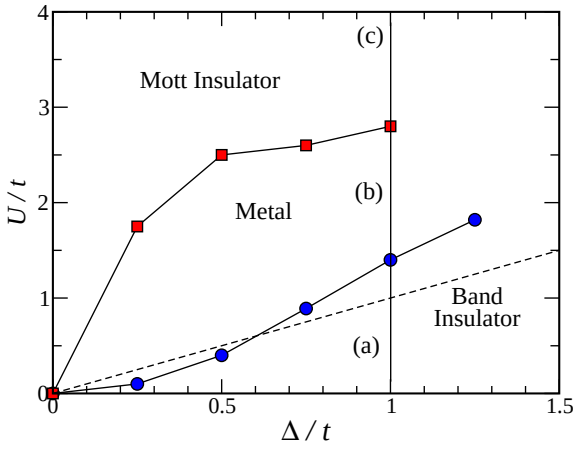

FIG. 2: The phase diagram of the ionic Hubbard model[16]. Symbols are the result of QMC simulations. The dashed line is the strong coupling ($t = 0$) phase boundary between band and Mott insulators. Points (a), (b) and (c) located, respectively, in the BI, the intermediate phase, and the MI are used in Fig. 3.

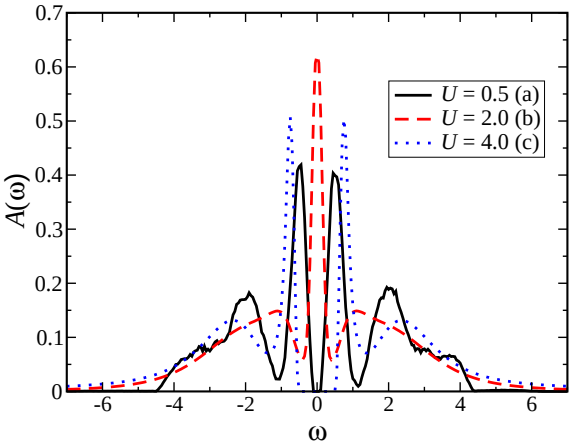

FIG. 3: Spectral function $A(\omega)$ for various values of interaction strength U with $\Delta = 1$ on a 6×6 lattice at $\beta = 12$ at half-filling. The letters (a)-(c) correspond to points on the phase diagram Fig. 2. Point (b) exhibits a metallic behavior as $A(\omega)$ is nonvanishing for $\omega = 0$. $A(\omega)$ exhibits clear gaps for points (a) and (c) which are, respectively, band and Mott insulating states.

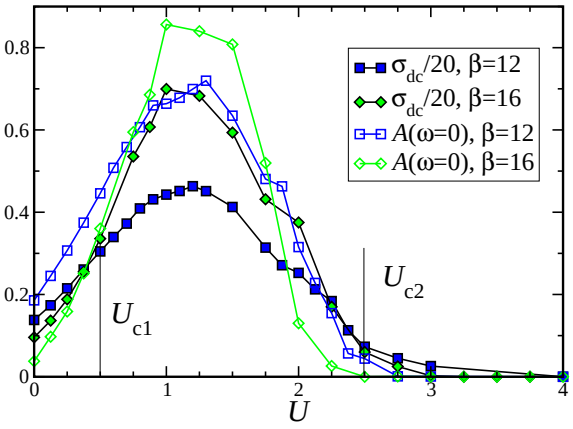

FIG. 4: The spectral function $A(\omega)$ and conductivity $\sigma_{\rm dc}$ are shown as functions of U at $\beta = 12$ and 16, at half-filling, and for $\Delta = 0.5$. There is a BI-metal transition at $U_{c1} \simeq 0.5$ and a metal to MI transition at $U_{c2} \simeq 2.5$.

minant is no longer always positive at half-filling resulting in a sign problem which can be severe.

The remaining sum over the HS field and the evaluation of observables is achieved by a Metropolis Monte Carlo algorithm. It is difficult to obtain good estimates for the observables when the determinant is often negative, *i.e.*, when the mean value of the sign of the determinant is small. This problem is important for intermediate values of U and Δ, while it is not severe in the limiting cases where we retrieve simple BI or MI phases (U or Δ small or large).

With this formulation, space and (imaginary-)time separated Green functions

$$G(\mathbf{R}, \tau) = \left\langle c_{\mathbf{r}+\mathbf{R}\sigma}(\tau)\, c^{\dagger}_{\mathbf{r}\sigma}(0) \right\rangle$$

are easily expressed as elements of the matrices. ¿From the spatial Fourier transform of $G(\mathbf{R}, \tau)$, one can extract the spectral function (essentially the density of states), by inverting the Laplace transform

$$G(\mathbf{k} = 0, \tau) = \int d\omega \, \frac{e^{-\omega\tau}}{1 + e^{-\beta\omega}} A(\omega). \qquad (2)$$

Solving for $A(\omega)$ remains a non-trivial task that is performed with a method of analytic continuation[23]. We measure correlation functions for charge and spin density waves (CDW and SDW, respectively), given by

$$C_{\substack{\rm cdw \\ \rm sdw}}(\mathbf{R}) = \frac{1}{N} \sum_{\mathbf{r}} \left\langle [n_{\mathbf{r}+\mathbf{R}\uparrow} \pm n_{\mathbf{r}+\mathbf{R}\downarrow}] \, [n_{\mathbf{r}\uparrow} \pm n_{\mathbf{r}\downarrow}] \right\rangle$$

where $+$ corresponds to CDW and $-$ to SDW. The staggered potential imposes a checkerboard modulation on the density, not only in the BI phase but in all phases as it breaks explicitly the translational invariance. Antiferromagnetic magnetic correlations are also expected in the MI phase. Thus, for both types of correlations, we expect ordering with a wave vector $\mathbf{k}_\pi = (\pi, \pi)$, characterized by the divergence of corresponding structure factors

$$S_{\substack{\rm cdw \\ \rm sdw}} = \sum_{\mathbf{R}} e^{i\mathbf{k}_\pi \cdot \mathbf{R}} C_{\substack{\rm cdw \\ \rm sdw}}(\mathbf{R}). \qquad (3)$$

IV. SPECTRAL FUNCTION, MAGNETIC AND CHARGE ORDERS

To complete our previous analysis[15] of the intermediate phase shown in Fig. 2 we evaluated the charge and spin correlations and spectral function. When the size is not explicitly mentioned, we used a $N = 6 \times 6 = 36$ sites lattice. $N_x = \sqrt{N}$ denotes the side of the lattice.

Fig. 3 shows the spectral function for $\Delta = 1$ (along the vertical line shown in Fig. 2) at $\beta = 12$ and for three values of U corresponding to the three different phases. For $U = 0.5$ and $U = 4$, corresponding to the BI and MI phases, the spectral function shows a gap around $\omega = 0$, thus indicating an insulator. In contrast, the spectral function for $U = 2$ is non zero and shows a quasi-particle peak at $\omega = 0$ which indicates metallic behavior.

These results are consistent with measurements of the conductivity in our previous article, as is confirmed by the direct comparison of the spectral function at zero frequency $A(\omega = 0)$ and the conductivity $\sigma_{\rm dc}$ shown in Fig. 4. For $\Delta = 0.5$ and as U is increased, the behaviors of these two quantities are similar: they both show, for intermediate values of U, a peak that grows with β. The ranges of interaction where there are peaks are slightly different because of finite size effects.

U_{c1} and U_{c2} are the critical repulsion energies that cause BI to metal and metal to MI phase transitions for a fixed value of Δ. These critical values are obtained by a finite temperature analysis of the conductivity[15]. As the

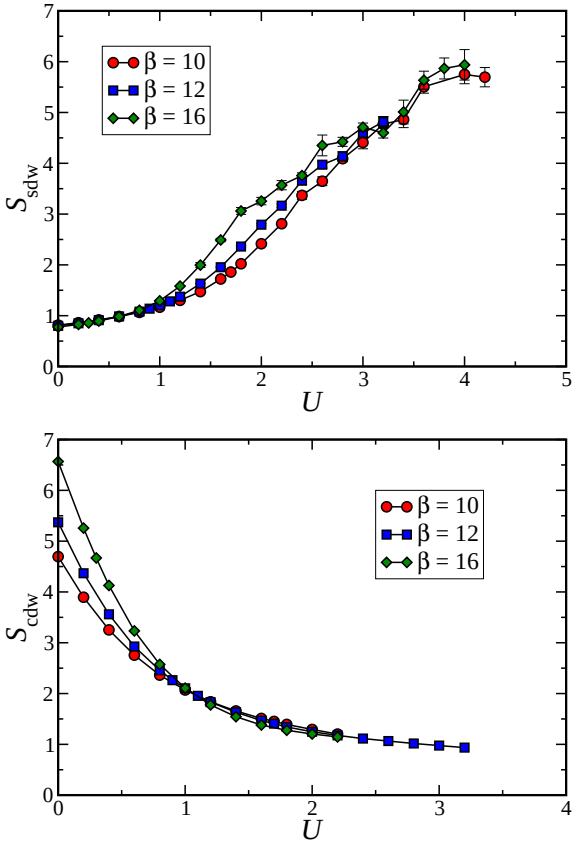

FIG. 5: Top: Antiferromagnetic structure factor $S_{\rm sdw}$ as a function of repulsion U shows antiferromagnetic order developing for large U. Bottom: Conversely, the charge structure factor $S_{\rm cdw}$ decreases as U increases. $\Delta = 0.25$ in both figures.

temperature is lowered, the conductivity increases in a metal and decreases in an insulator. Locating the points where the behavior of the conductivity changes gives the critical values. For $\Delta = 0.5$, the BI-metal transition is located at $U_{c1}/t \simeq 0.5$, the metal-MI transition is located at $U_{c2}/t \simeq 2.5$ and the metallic region is in between.

Structure factors $S_{\rm sdw}$ and $S_{\rm cdw}$ are shown in Fig. 5 for Δ= 0.25 and for inverse temperatures $\beta = 10, 12$ and 16. For these values of Δ, the metallic boundaries are $U_{c1} \simeq 0.1$ and $U_{c2} \simeq 1.7$. As U is increased, $S_{\rm sdw}$ increases as the system is driven towards the MI phase, while $S_{\rm cdw}$ decreases, in moving away from the BI phase. The transitions in these quantities when we cross the phase boundaries are not sharp on lattices of fixed, finite size owing to finite size rounding effects. In addition, as stated above, a smoother evolution is expected for $S_{\rm cdw}$ as a modulation of ρ is imposed by the external potential for all parameter values.

In a conventional Hubbard model, the MI at half filling is always an antiferromagnet. However, it has been suggested recently for related models[17] that the metal-MI and para- to antiferro-magnetic (PM-AF) transitions may not take place together. A finite size scaling analysis of $S_{\rm sdw}$ for different values of U is needed to check

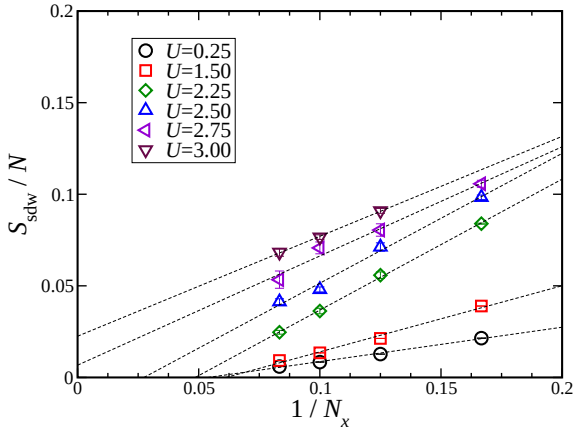

FIG. 6: The antiferromagnetic structure factor $S_{\rm sdw}/N$ as a function of inverse lattice size $1/N_x$ at $\Delta = 0.5$ and $\beta = 12$ for various U. The different values of U correspond to different phases: $U = 0.25$ to the BI, $U = 1.50, 2.25$ and 2.5 to the metal, and $U = 2.75$ and 3 to the MI. The lines are least-squares fit to the data and the extrapolation leads to the value of $S_{\rm sdw} = m2/3$ for an infinite system. There is antiferromagnetic long range order only in the MI phase.

whether these two boundaries coincide in our model. The structure factor $S_{\rm sdw}$ increases like the number of sites N in the thermodynamic limit

$$\frac{S_{\rm sdw}}{N} = \frac{m^2}{3} + O\left(\frac{1}{N_x}\right) \qquad (4)$$

where $m2$ is the antiferromagnetic order parameter. Fig. 6 shows structure factors for sizes up to $N = 12 \times 12$ sites for different values of U. Δ is set to 0.5 and the metallic phase appears between $U_{\rm c1} \simeq 0.5$ and $U_{\rm c2} \simeq 2.5$. We apply a least squares fit to the data, and extrapolate to an infinite system. We find a non-vanishing structure factor only in the MI phase ($U = 2.75$ and 3). In all the other cases, including points located close to the metal-MI transition ($U = 2.25$ and 2.5), the structure factor goes to zero as the size is increased.

The PM-AF transition, therefore, takes place between $U = 2.5$ and $U = 2.75$ and appears to be simultaneous with the metal-MI transition. Although our study on limited sizes cannot completely exclude completely the possibility of an exotic AF metallic phase located around the metal-MI boundary, our data suggest that it does not occur.

V. AWAY FROM HALF-FILLING

We extend our study to determine the behavior away from half-filled band. In Fig. 7, the density ρ is plotted as a function of chemical potential. The compressibility κ is given by $\partial\rho/\partial\mu$. For κ=0, incompressible insulating phases are present which is indicated by plateaux in the ρ versus μ curve. Both the MI ($U = 2.0, \Delta = 0.2$) and BI

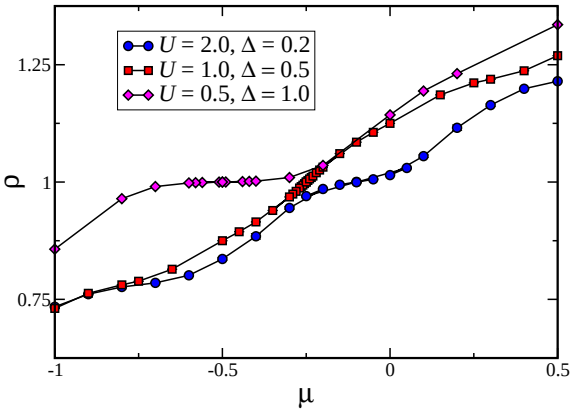

FIG. 7: Density, ρ, as a function of chemical potential μ for the different phases. The Mott ($U = 2.0, \Delta = 0.2$, circles) and band ($U = 0.5, \Delta = 1.0$, diamonds) insulating phases have plateaux as the compressibility $\kappa = \partial\rho/\partial\mu = 0$ at half-filling. For the metallic phase ($U = 1.0, \Delta = 0.5$, squares), there is no plateau in the region around $\rho = 1$.

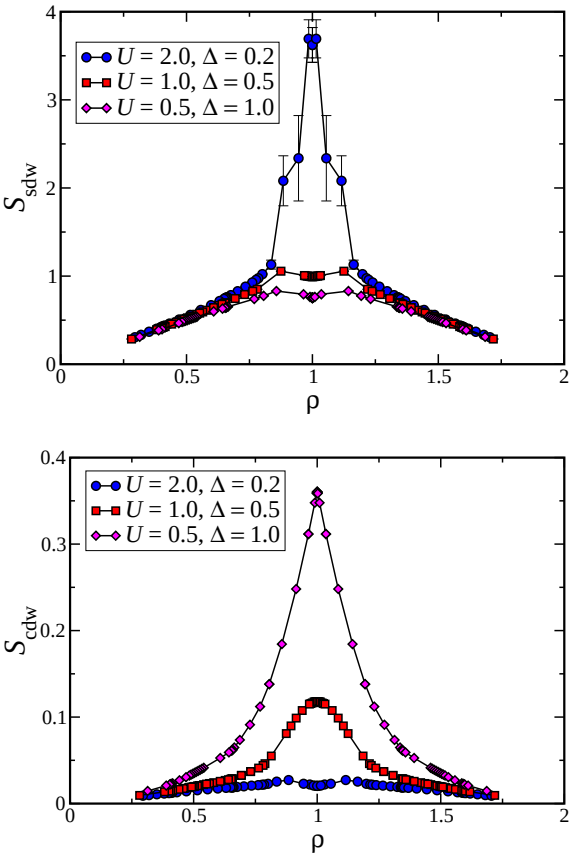

FIG. 8: Spin (top) and charge (bottom) structure factors as functions of density. The parameters are the same as in Fig. 7. As ρ approaches half-filling, $S_{\rm sdw}$ reaches its maximum value for the Mott phase. Conversely, $S_{\rm cdw}$ is maximum at $\rho = 1$ for the band insulator. The metallic phase has a slight peak in $S_{\rm cdw}$ but not in $S_{\rm sdw}$.

($U = 0.5, \Delta = 1.0$) phases have this distinctive plateau at half-filling. The metallic nature of the intermediate phase is once again confirmed by the absence of a plateau around $\rho = 1$.

Using the same parameters U and Δ, we show in Fig. 8 the evolution of the structure factors as functions of ρ. As expected, for the parameters corresponding to the MI at $\rho = 1$, $S_{\rm sdw}$ shows a strong peak around half-filling indicating the presence of the AF-MI in this case and its rapid suppression upon doping. In this case, charge correlations always remain small, as double occupancy of sites is essentially forbidden. Similarly, for the parameters corresponding to the BI, the peak is present in $S_{\rm cdw}$ at $\rho = 1$ and $S_{\rm sdw}$ remains small for all densities, as the occupation of larger energy site is suppressed. For the metallic case, there is no peak in the magnetic structure factor at $\rho = 1$ but a moderate peak in $S_{\rm cdw}$.

In all these three cases, away from half-filling, the structure factors are rapidly suppressed and the system is compressible and becomes a paramagnetic metal.

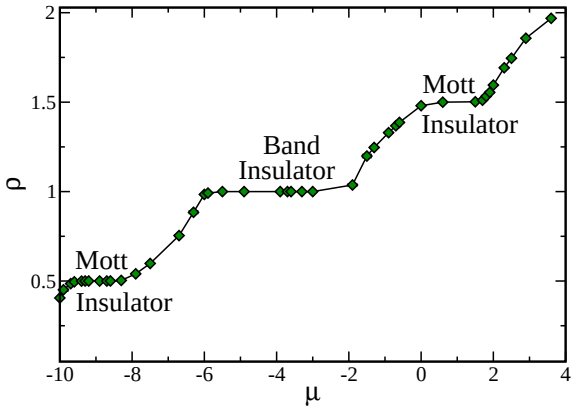

FIG. 9: The density, ρ, as a function of chemical potential μ for $\Delta = 8$ and $U = 4$ at $\beta = 10$. The plateaux represent the various insulating phases. The regions where $\kappa > 0$ are metallic phases.

For stronger interactions and staggered potential, other ordered phases can be found at quarter and three quarters fillings. For $U = 4$ and $\Delta = 8$, there is a band insulator at half-filling shown by the $\rho = 1$ plateau in Fig. 9. Additional plateaux emerge at $\rho = 0.5$ and 1.5. The plateau at $\rho = 0.5$ corresponds to a state where all the lower energy sites are occupied by one fermion. Adding a fermion to an already occupied site increases the energy approximately by U, while adding it to an empty (high energy) site increases it by Δ. There is then an energy gap, roughly equal to the smaller of the two parameters (U in this case). We then have a Mott insulator at quarter filling and, symetrically, another one at three quarters filling. In the case where U is larger than Δ, the situation is reversed and we expect a MI at half-filling and a BI for $\rho = 0.5$ and $\rho = 1.5$ (this case is difficult to treat numerically because of a strong sign problem).

Although the system is incompressible for $\rho = 0.5$,

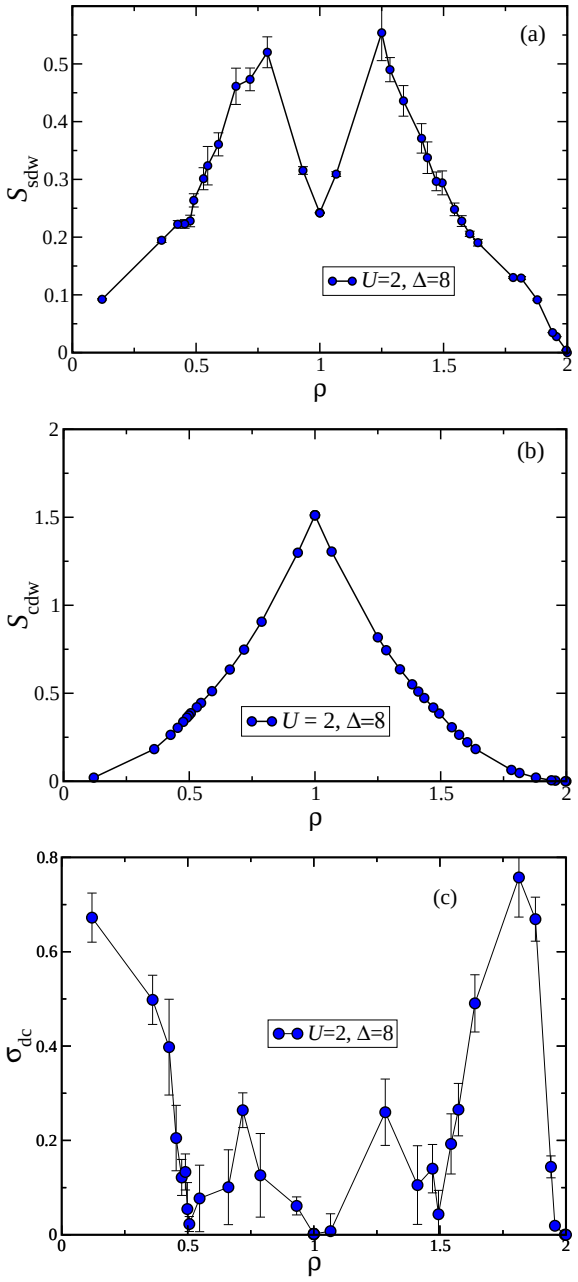

FIG. 10: (a) Antiferromagnetic structure factor $S_{\rm sdw}$, (b) charge structure factor $S_{\rm cdw}$ and (c) conductivity, $\sigma_{\rm dc}$ as functions of ρ at $U = 2$, $\Delta = 8$ and $\beta = 10$. Note that $\sigma_{\rm dc}$ vanishes in the three solid phases, $\rho = 1/2$, 1, 3/2.

there is no concommitant magnetic order: in Fig. 10, $S_{\rm sdw}$ always remains small as ρ is varied away from half-filling and there is no AF peak around quarter filling (the maximum being around $\rho = 0.75$). The AF ordering appears when the fermions jump between neighboring sites, thus creating an effective antiferromagnetic coupling between spins. At quarter filling, the particles are surrounded by empty sites and there is no effective coupling. As for $S_{\rm cdw}$ we only observe a peak at half-filling (Fig. 10). A plot of the conductivity (Fig. 10(c)) versus ρ shows that, indeed, $\sigma_{\rm dc}$ vanishes for $\rho = 1/4$ and $\rho = 3/4$ corresponding to the plateaux observed in Fig. 9.

VI. BOND-ORDERED WAVES

Long range Bond-ordered waves (BOW) are known to exist in one dimension in the ionic Hubbard model[6,7,8] as well as in other one-dimensional systems exhibiting density modulation such as extended Hubbard models[10,11]. (In the latter case, the two numerical treatments, using the stochastic series expansion[11] and density matrix renormalization group[10], disagree on the precise width of the BOW phase as well as over what range of coupling values it is present.) It was suggested by Kancharla *et al.*[14] that the intermediate phase observed at half-filling in the two-dimensional case studied here was in fact a bond-ordered state, as in one dimension. Other studies have attempted to observe bond-order in two dimensions, for example in extended Hubbard models[24]. In two dimensions, bond orders have mostly been obtained in Hamiltonians possessing rather special geometries or interactions, e.g. on checkerboard lattices[25] or by including additional terms such as ring exchanges[26].

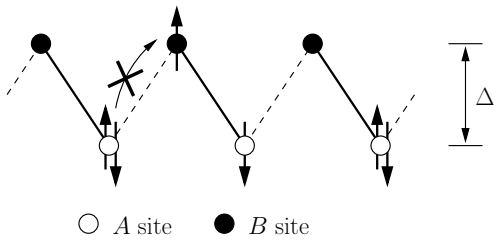

FIG. 11: Schematic diagram of how a bond-ordered wave occurs in one dimension. For $U \sim \Delta$ both large, the electrons may move to a site of higher chemical potential as shown with the spin-up electron. The spin-down electron in the left well is not likely to move to the right because it will cost a large energy Δ to doubly occupy the site of higher chemical potential. Prohibited movement to left causes a decrease in kinetic energy for that bond. This alternation of two bonds with weak and strong kinetic energy bonds is an indication of the appearance of a bond order. Strong bonds are continuous thick lines, weak bonds are dotted lines.

Hence, bond order seems in general more difficult to obtain in two dimensions than in one. In our system, we can understand this with the argument sketched in Fig. 11. Starting from a situation where all the particles are located on the low energy sites (A sites), a jump to a high energy site (B site) increases the energy roughly by $\Delta - U$. If Δ and U are of the same order of magnitude, this energy cost is small and the jump has a high probability to happen. This B site is connected to two A sites: the one where the jumping particle comes from (to the right in Fig. 11) and another one (to the left) still occupied by two particles. The jumps on the left bond

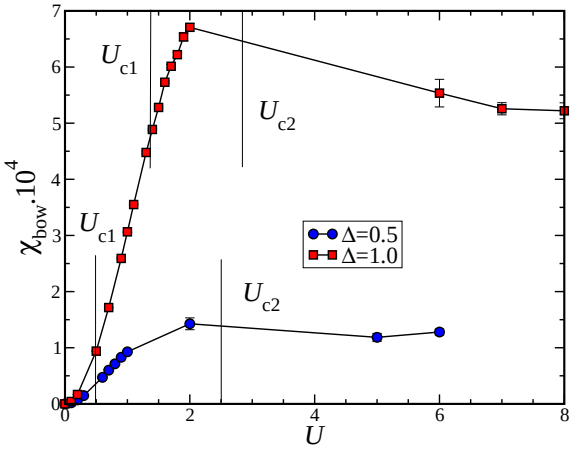

FIG. 12: The bond-ordered susceptibility as a function of U at $\rho = 1$ for $N = 12 \times 12$ and $\beta = 10$. The vertical lines separate the three different phases for two different values of the staggered potential. The maximum of this bond-order parameter is in the metallic region but is of order 10^{-4}.

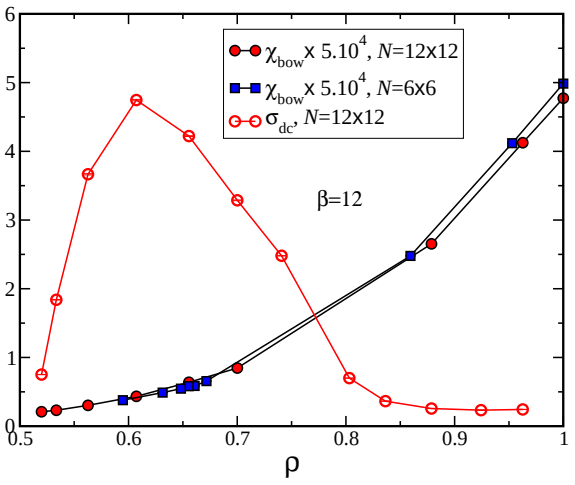

FIG. 13: The bond-ordered susceptibility and conductivity as functions of ρ for $\Delta = 1$, $U = 0.5$, and $\beta = 12$. Doping away from half-filling, the susceptibility is non-zero even when the band is only partially full and the system is unquestionable metallic.

are suppressed: the particle on the B site and the particle having the same spin (an up spin in the sketch) on the A site cannot jump because of Pauli principle, while a jump of the remaining particle has a large energy cost Δ.

In short, having a particle jumping on a bond (and thus a contribution to the kinetic energy on this bond) will inhibit jumps on the following bond. In one dimension, this can lead to a bond order with alternate strong and weak values of the kinetic energy. On a two dimensional square lattice, the appearance of a strong bond will inhibit the three other bonds linked to the same site and it seems more difficult to generate regular arrays of weak and strong bonds.

To check if there is a BOW, we examined the correlation function of the kinetic energy

$$K^{xx}(\mathbf{R}) = \sum_{\mathbf{r}} \langle k^x_{\mathbf{r}+\mathbf{R}} k^x_{\mathbf{r}} \rangle,$$

where $k^x_{\mathbf{r}}$ is the kinetic energy operator connecting sites $\mathbf{r}$ and $\mathbf{r} + \hat{x}$ ($\hat{x}$ being a unit vector directed along the x direction),

$$k^x_{\mathbf{r}} = \sum_{\sigma=\uparrow,\downarrow} (c^\dagger_{\mathbf{r}+\hat{x},\sigma} c_{\mathbf{r},\sigma} + c^\dagger_{\mathbf{r},\sigma} c_{\mathbf{r}+\hat{x},\sigma}).$$

The Fourier transform of $K^{xx}(\mathbf{R})$ always exhibits a very small peak for $\mathbf{k}_\pi = (\pi, \pi)$, in all the different phases at or away from half-filling. Finite size scaling analysis indicates that these peaks persist in large size lattices, but this is the case for all the different phases, not only in the intermediate phase. We also studied the BOW susceptibility[11] for this wave vector

$$\chi_{\rm bow} = \sum_{\mathbf{R},\mathbf{r},\tau} e^{i\,\mathbf{k}_\pi \cdot \mathbf{R}} \left\langle k^x_{\mathbf{r}+\mathbf{R}}(\tau) k^x_{\mathbf{r}}(0) \right\rangle \qquad (5)$$

Fig. 12 shows the evolution of $\chi_{\rm bow}$ at half-filling as a function of U and for two different values of Δ. The curve is maximum in the intermediate phase but is also non zero in other phases. Similar results are obtained for bonds oriented along the y direction and for mixed x-y cases.

We do not believe these signals to indicate the presence of a BOW phase for the following reasons (a) The values obtained are extremely small. (b) These "BOW signals" are ubiquitous in *all three phases* and not specific to the intermediate one. The susceptibility is, for example, nearly as important in the MI phase as in the intermediate phase. As soon as U and Δ are both non-zero, we observe this very weak non-zero value of $\chi_{\rm bow}$. (c) Starting from the metallic phase ($U = 0.5, \Delta = 1$) and doping away from half-filling the system is certainly known to be metallic (see Fig. 13) yet the BOW susceptibility is non zero and comparable to the value found at half-filling. For all these reasons, we believe that these tiny signals are only a weak signature of an interplay between the interaction and externally imposed checkerboard potential.

VII. CONCLUSIONS

We have extended our previous study of the phase diagram of the ionic Hubbard model[15]. In addition to new QMC results for the conductivity, we calculated the spectral function, the kinetic energy correlation function (the order parameter for the BOW phase) and the magnetic and charge order parameters. Our results point to the presence of a normal conducting metallic phase intervening between the band and Mott insulating phases. In particular, we have not found a clear signal in the BOW

order parameter and susceptibilities indicating the presence of such a phase.

We also studied the system doped away from half filling. When the band or Mott insulating phase is doped, a conducting phase is obtained except at fillings of 1/4 and 3/4 where we found insulating phases without magnetic order.

G.G.B., F.H., and K.B. are supported by a grant from the CNRS (France) PICS 18796, R.T.S. and N.P. were supported by NSF ITR 0313390. We acknowledge helpful discussions with M.M. Gibbard.

[1] N. Nagaosa and J. Takimoto, J. Phys. Soc. Jpn **55**, 2735 (1986) ; *ibid.* **55**, 2745 (1986) ; *ibid.* **55**, 2745 (1986) and references therein.

[2] T. Egami, S. Ishihara and M. Tachiki, Science **261**, 130 (1994).

[3] S. Ishihara, T. Egami and M. Tachiki, Phys. Rev. B **49**, 8944 (1994).

[4] J. Hubbard and J.B. Torrance, Phys. Rev. Lett. **47**, 1750 (1981).

[5] T. Wilkens and R.M. Martin, Phys. Rev. B **63**, 235108 (2001); M.E. Torio, A.A. Aligia, and H.A. Ceccatto, Phys. Rev. B **64**, 121105(R) (2001); C.D. Batista and A.A. Aligia, Phys. Rev. Lett. **92**, 246405 (2004); G.I. Japaridze, R. Hayn, P. Lombardo, and E. Müller-Hartmann, cond-mat/0611415 (2006).

[6] A. P. Kampf, M. Sekania, G. I. Japaridze, and Ph. Brune, J. Phys.: Condens. Matter **15** 5895-5907 (2003).

[7] Y.Z. Zhang, C.Q. Wu, and H.Q. Lin, Phys. Rev. B **67**, 205109 (2003).

[8] S.R. Manmana, V. Meden, R.M. Noack, and K. Schöhammer, Phys. Rev. B **70**, 155115 (2004).

[9] A.A. Aligia and C.D. Batista, Phys. Rev. B **71**, 125110 (2005).

[10] E. Jeckelmann, Phys. Rev. Lett. **89**, 236401 (2002).

[11] P. Sengupta, A.W. Sandvik, and D.K. Campbell, Phys. Rev. B **65**, 155113 (2002).

[12] H. Craig, C.N. Varney, W.E. Pickett, and R.T. Scalettar, work in progress.

[13] A. Garg, H.R. Krishnamurthy, and M. Randeria, Phys. Rev. Lett **97** 046403 (2006).

[14] S.S. Kancharla and E. Dagotto, Phys. Rev. Lett. **98**, 016402 (2007).

[15] N. Paris, K. Bouadim, F. Hébert, G.G. Batrouni, and R.T. Scalettar, Phys. Rev. Lett. **98**, 046403 (2007).

[16] Our previous article[15] contained a factor of two error in the value of the staggered potential Δ. The correct definition of the Hamiltonian is the one given here. The BI-MI transition line in the $t = 0$ limit in Fig. 2 has been modified accordingly.

[17] S.S. Kancharla and S. Okamoto, cond-mat/0703728.

[18] L. Craco, P. Lombardo, R. Hayn, G.I. Japaridze, and E. Müller-Hartmann, cond-mat/0703814.

[19] K. Maitim, R. Shankar Singh, and V.R.R. Medicherla, cond-mat/0704.0327.

[20] S.S. Kancharla and E. Dagotto, Phys. Rev. B **74**, 195427 (2006); S. Okamoto and A.J. Millis, Phys. Rev. B **70**, 075101 (2004).

[21] K. Byczuk, W. Hofstetter, and D. Vollhardt, Phys. Rev. B **69**, 045112 (2004); P. Lombardo, R. Hayn, and G.I. Japaridze, Phys. Rev. B **74**, 085116 (2006); N. Paris, A. Baldwin, and R.T. Scalettar, cond-mat/0607427 (2006).

[22] S.R. White, D.J. Scalapino, R.L. Sugar,E.Y. Loh, J.E. Gubernatis, and R.T. Scalettar, Phys. Rev. B **40**, 506 (1989).

[23] A.W. Sandvik, Phys. Rev. B **57**, 10287 (1998).

[24] M. Murakami, Journal of the Physical Society of Japan **69**, 1113 (2000)

[25] M. Indergand, C. Honerkamp, A. Laüchli, D. Poilblanc, and M. Sigrist, Phys. Rev. B **75**, 045105 (2007).

[26] R.G. Melko, A.W. Sandvik, and D.J. Scalapino, Phys. Rev. B **69**, 100408 (2004).